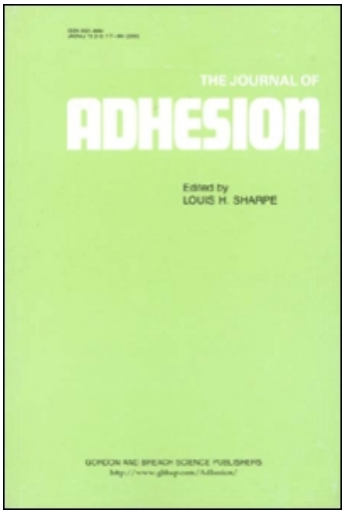

The Journal of Adhesion
Publication details, including instructions for authors and subscription information:
http://www.informaworld.com/smpp/title~content=t713453635

Particle-Surface Collision Dynamics: What Might They Tell Us?

B. Dahneke[a]
[a] Eastman Kodak Company, Rochester, NY, USA

To cite this Article Dahneke, B.(1995) 'Particle-Surface Collision Dynamics: What Might They Tell Us?', The Journal of Adhesion, 51: 1, 125 — 137
To link to this Article: DOI: 10.1080/00218469508009993
URL: http://dx.doi.org/10.1080/00218469508009993

J. Adhesion, 1995, Vol. 51, pp. 125–137
Reprints available directly from the publisher
Photocopying permitted by license only

Particle-Surface Collision Dynamics: What Might They Tell Us?*

B. DAHNEKE

Eastman Kodak Company, Rochester, NY 14652-3712, USA

(Received March 24, 1995; in final form May 5, 1995)

Particle-surface collisions have broad influence in various processes of interest in science and technology. A simple, conservation-of-energy model has been proposed[1, 2] for characterizing the *simplest particle-surface-collision*, namely, the idealized collision of a homogeneous, solid, non-rotating particle (such as a sphere) moving at normal incidence towards a flat, smooth surface of a solid body in vacuum. Dahneke,[3] Hays and Wayman,[4] and Wall *et al.*[5] measured particle-surface collisions approaching this simplest one. We describe an extensive set of measured collision data for 1.27 μm diameter polystyrene spheres striking a polished, fused-silica surface at normal incidence, in vacuum, over a broad range of particle-approach velocities and use the data to test the model. The goal is to determine the level of agreement between the measured data and the predictions of the model and what information may be obtained by the combination of data and model. We find the model fits the measured data well and the combination provides a number of particle-surface properties including the coefficient of restitution, the increase in attractive potential energy during collision, the impact energy (material stress) at onset of particle deformation, and possibly other properties.

KEY WORDS polystyrene spheres; incident and rebound velocities; coefficient of restitution; particle-surface properties; attractive potential energy during collision; impact energy (material stress); particle deformation; conservation of energy model.

INTRODUCTION

Particle-surface collisions are important in scientific research, engineering design and development, environmental and public health monitoring, and manufacturing and product quality and reliability assurance. Several processes within these categories and others have important economic consequences, including fouling, contamination, erosion, mechanical failure, manufacturing and process control, sampling, and diagnostics. As one example, particle-surface-system processes are influenced by certain material properties best determined from measured collision dynamics between test or sample particles and surfaces. Measured data and a valid model of particle-surface collisions would appear to be useful across a range of applications. These topics are addressed in this study.

Dahneke,[3] Hays and Wayman,[4] and Wall *et al.*[5] have measured particle-surface collisions approaching the simplest ones (described in the abstract). One set of methods[3] is of particular interest to the present investigation, because the data

*Presented in part at the Seventeenth Annual Meeting of The Adhesion Society, Inc., in Orlando, Florida, U.S.A., February 21–23, 1994.

described here were obtained thereby and because the set provides accurate, simple-collision data over a broad range of normal-incident particle velocities relative to a target surface in vacuum under precisely controlled conditions. These data do not require calculated corrections to account for air drag and can be used to follow particle motion through a collision process without uncertainty due to fluid friction in a quiescent or moving fluid near a surface.

We use a set of 763 measured particle-surface-collision data points, from which 639 are selected as most accurate. The data are all for a single-particle species, namely, nearly uniform polystyrene spheres of 1.27 μm mean diameter and 1.13 pg mean mass, striking a polished, fused-silica surface at normal incidence in vacuum. The data consist of jointly-measured particle incident and rebound velocities normal to the target surface at particle-surface separations sufficiently large so that interactions are negligible. However, in a vacuum environment where free particles undergo ballistic motion, their motion near another body can be inferred from "far-field" motion data in terms of a *particle-surface interaction function* and Newton's second law of motion. Conversely, such data provide a means for interrogating particle-surface interactions and the many aspects of a particle- surface collision process. We seek to discover in this study what particle-surface collision dynamics measured in the far field might tell us about collision-process physics, attractive interactions, and material properties.

We describe in section II a simple, quasi-stationary, conservation-of-energy model[1,2] for characterizing simple, particle-surface collisions. In section III we summarize the measurement method used and the particle-surface collision data obtained by it. In section IV we combine the measured data and the model to discover what information the particle-surface collision dynamics might reveal about a particle-surface system. In the final section, section V, we summarize conclusions resulting from the investigation.

II SIMPLE CONSERVATION-OF-ENERGY MODEL FOR PARTICLE-SURFACE COLLISIONS

A simple, quasi-stationary collision of a particle and a surface is illustrated by the schematic curves of Figure 1 showing particle-surface interaction force, $F(x)$, *versus* normal direction displacement, x. Although exaggerated for clarity, these curves are typical of those measured by Burnham *et al.*[6,7] for force *versus* displacement of the tip of an atomic-force-microscope probe slowly moved in a normal direction towards a solid surface and then slowly retracted in a direction normal to the surface. The hysteresis in these curves represents *total energy dissipated during collision*, $W = KE_{i\infty} - KE_{r\infty}$. W results from a difference in interaction force *versus* displacement for the incident and rebound states, due to causes which include temporary and permanent (plastic) deformation, making or breaking of chemical bonds, change in electrostatic nature of the system by contact charging, etc. As a consequence, the minimum (negative) attractive forces for the incident and rebound directions, identified as points (b) and (c) in Figure 1, may differ and are denoted the *attractive* and *adhesive* forces. (Other particle-surface separations may be selected in the model, subject to a single constraint described below).

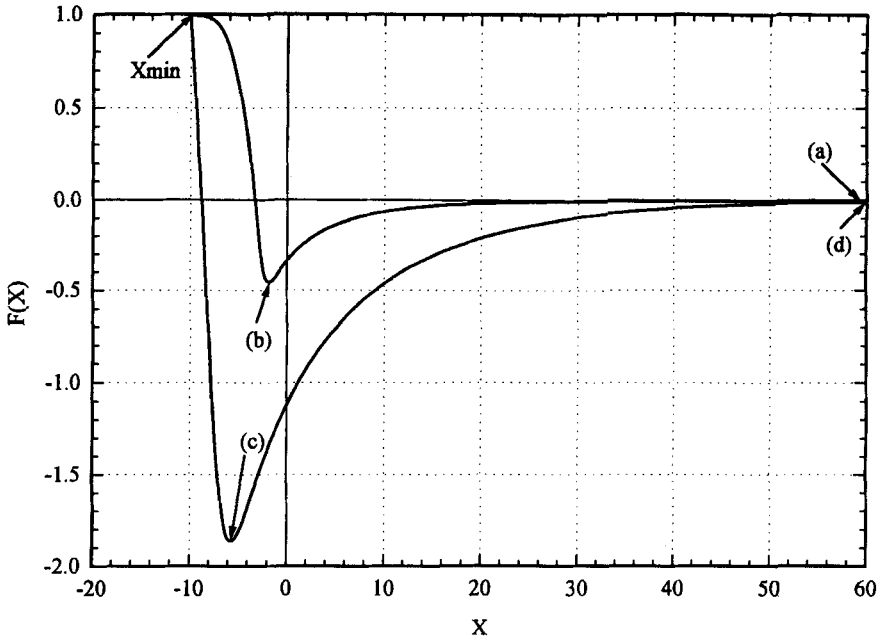

FIGURE 1 Schematic plots of particle-surface-interaction force *versus* incident- and rebound- direction displacement [after measured data of Burnham *et al.* Refs. 6 and 7 of force on an atomic-force-microscope tip *versus* tip displacement from a test surface]. Hysteresis in the force *versus* displacement cycle provides kinetic energy dissipated during impact. The minimum values of the incident- and rebound-direction force curves occur at separations x_{io} (at *b*) and x_{ro} (at *c*), respectively, and are denoted the attractive and adhesive forces (F_{io} and F_{ro}), with $x_{ro} < x_{io}$ due to plastic or temporary dynamic deformation. Four system separation states are indicated, two each for incident ($a + b$) and rebound ($c + d$) direction motions (see text). Minimum separation, x_{min}, is indicated with negative separation being the apparent inter-penetration, or simply penetration, of the initial, *undeformed* shapes of the bodies.

In a quasi-stationary, particle-surface collision illustrated in Figure 1, the quasi-stationary model[1, 2] considers impact kinetic energy to be *irreversibly* dissipated over only the inbound interval from x_{io} [point (b)] to x_{min} and the outbound interval from x_{min} to x_{ro} [point (c)]. These intervals are the ones of highest stress and strain levels and rates-of-change and are the intervals over which the influence of (irreversible) dynamic dissipation mechanisms and plastic deformation are expected.

We, therefore, stipulate a constraint on the model that all irreversible energy exchange must occur "inside" (to the left of) points (b) and (c) for incident and rebound states, respectively. That is, separations x_{io} [at (b)] and x_{ro} [at (c)] must lie on or beyond the separation limits beyond which energy exchange is conservative, for which the relation between separation, kinetic and potential energy is simply and fully characterized by the interaction potential energy function, $\varphi(x)$. When this constraint is satisfied, (b) and (c) can be specified as the separations at the attractive- and adhesive-energies and all exchange between kinetic and potential energy at or beyond (b) and (c) is conservative and reversible. In this case, the attractive energies, E_i and E_r, of the model can be sought by fitting it to measured data. On the other hand, when this constraint is

not satisfied at specified separations x_{io}, x_{ro}, one or both must be increased, *i.e.*, interaction energies E_i and E_r must be reduced from the actual stationary values, due to a model dependence of these quantities. Thus, *E_i and E_r determined by this model are expected to be either equal to or smaller than the quasi-stationary E_i and E_r values.*

The model is, therefore, based on a simple, quasi-stationary, particle-surface collision characterized by the total, particle-surface-system energy. From this principle follows an equation relating particle kinetic energy, particle-surface potential energy and (irreversible) net work of collision at four particle-surface separations, *viz.*, (a) large, incident-state separation, $x_{i\infty}$, (b) intermediate incident-state separation, x_{io} [at which interaction energy is $\varphi_i(x_{io})$], (c) intermediate rebound-state separation, x_{ro} [at which interaction energy is $\varphi_r(x_{ro})$] and (d) large, rebound-state separation, $x_{r\infty}$. In the model, we regard all transitions as energetically reversible except for the transition (b) → (c), in which partially- or wholly-irreversible energy dissipation occurs. With $W_{i\to j}$ denoting net collision work between separation states i and j, the conservation-of-energy expression is[1]

$$KE_{i\infty} = KE_{io} + E_{io} + W_{a\to b} = KE_{ro} + E_{ro} + W_{a\to c} = KE_{r\infty} + W_{a\to d}, \tag{1}$$

where x_{jk} = particle-surface separation for motion-state j and separation-state k,
V_{jk} = magnitude of particle velocity for motion-state j and separation-state k,
Z = $KE_{i\infty}$ = independent variable used to characterize collision dynamics,
$KE_{i\infty}$ = $m \times V_{i\infty}^2/2$ = incident-state particle kinetic energy at $x_{i\infty}$,
KE_{io} = $m \times V_{io}^2/2$ = incident-state particle kinetic energy at x_{io},
KE_{ro} = $m \times V_{ro}^2/2$ = rebound-state particle kinetic energy at x_{ro},
$KE_{r\infty}$ = $m \times V_{r\infty}^2/2$ = rebound-state particle kinetic energy at $x_{r\infty}$,
$E(x)$ = $\varphi(x)$ = particle-surface interaction potential energy at separation x,
E_{io} = $-\int_{x_{io}}^{x_{i\infty}} \varphi_i'(x)\,dx$ = incident-state interaction potential energy at x_{io},
E_{ro} = $-\int_{x_{ro}}^{x_{r\infty}} \varphi_r'(x)\,dx$ = rebound-state interaction potential energy at x_{ro},
$E_{i\infty}$ = $E_{r\infty} = 0$, by definition (i.e., interaction energy $\varphi(x) \to 0$ as $x \to \infty$),
ΔE_0 = $E_{r0} - E_{io}$ = interaction energy difference at state/separation x_{ro} and x_{io},
W_0 = $W_{b\to c} = -\int_{x=x_{io}}^{x_{\min}} F_i(x)\,dx + \int_{x=x_{\min}}^{x_{ro}} F_r(x)dx = KE_{io} - KE_{ro} = W + \Delta E_0$,
W = $W_{a\to d} = KE_{i\infty} - KE_{r\infty} = W_o - \Delta E_0$ = energy dissipated during collision,
$F_i(x)$ = incident-state, particle-surface interaction force at separation x,
$F_r(x)$ = rebound-state, particle-surface interaction force at separation x.

Work of collision, W_0, and *coefficient of restitution*, e, are defined by

$$e^2 = KE_{ro}/KE_{io} = 1 - W_0/KE_{io}, \quad \text{where } W_0 = KE_{io} - KE_{ro}. \tag{2}$$

From (1) and (2), $KE_{ro} = KE_{r\infty} - E_{ro} = KE_{r\infty} - \Delta E_0 - E_{io}$, $KE_{io} = KE_{i\infty} - E_{io}$ and

$$e^2 = KE_{ro}/KE_{io} = 1 - (KE_{io} - KE_{ro})/KE_{io} = (KE_{r\infty} - \Delta E_0 - E_{io})/(KE_{i\infty} - E_{io}),$$

from which the magnitude of the velocity ratio far from the surface, where it is accessible to convenient measurement, is

$$V_{r\infty}/V_{i\infty} = \{e^2 + 2 \times [\Delta E_0 + (1 - e^2) \times E_{io}]/(m \times V_{i\infty}^2)\}^{1/2}, \tag{3}$$

and the capture limit velocity, defined[1] as the $V_{i\infty}$ at which $V_{r\infty}$ is zero by (3) [and the lower limit of $V_{i\infty}$ for which (1) and (3) are valid], is

$$V^*_{i\infty} = \{-2 \times [\Delta E_0 + (1-e^2) \times E_{io}]/(m \times e^2)\}^{1/2}. \quad (4)$$

Most of these equations were derived in the original description of the model[1] but without the details and comparison with data included here. In the case $|\Delta E_0| \gg |(1-e^2)E_{io}|$, $V_{r\infty}/V_{i\infty}$ and $V^*_{i\infty}$ approach the asymptotic limits

$$V_{r\infty}/V_{i\infty} = \{e^2 + 2 \times \Delta E_0/(m \times V^2_{i\infty})\}^{1/2},$$

and

$$V^*_{i\infty} = \{-2 \times \Delta E_0/(m \times e^2)\}^{1/2},$$

the expressions used by Wall *et al.*[5] Equations (1) through (4) and their descendants are used in this investigation to rationalize and "interrogate" measured particle-surface collision data.

III JOINTLY MEASURED $V_{i\infty}$ and $V_{r\infty}$ DATA

We show in Figures 2 through 6 the measured $V_{i\infty}$ and $V_{r\infty}$ data obtained in this study. These data are presented in the form $V_{r\infty}/V_{i\infty}$ versus $V_{i\infty}$ in Figures 2 through 4 and in the form $W = KE_{i\infty} - KE_{r\infty}$ *versus* $KE_{i\infty}$ in Figures 5 and 6. All points shown were measured for polystyrene spheres, narrowly distributed in diameter about a mean value of 1.27 μm and in mass about a mean value of 1.13 pg, bouncing on a fused-silica surface in vacuum. The measurement method has been previously described,[3] to which description the reader may refer for details. The method is only summarized here in two paragraphs. The data of Figures 2 and 5 each contain a total of 763 data points from which 639 points were selected by simple inspection of magnified plots as being "regularly close" to the local mean. Data from these 639 selected points are shown in Figures 3 and 4 and data from the 763 are shown in Figure 6. Differences in values fitted to the two data sets were generally insignificant.

The 1.27 μm diameter polystyrene spheres were nebulized from a water suspension and the water was evaporated from the particles and absorbed by a desiccant material through which the air-suspension of wet particles was passed. Because the water solution contained surfactant as a particle stabilizer, the dried particles were covered with a thin layer of organic surfactant material (probably sodium dodecyl sulfate).

After drying, the test particles were introduced along an axis normal to the target surface in a vacuum environment (10^{-4} torr) at selected incident velocity by[1] adiabatic expansion of an airborne suspension of the particles,[2] velocity modulation in a "braking chamber" in which air was maintained at a precisely controlled pressure to obtain a desired impact velocity,[3] collimation of the "particle beam" to insure normal direction incidence, and[4] impaction on the target. At separations of 2 and 3 cm from the target surface, each particle passed through a focused light beam, from a low-power (5 mW) HeNe laser. A pair of scattered light signals generated at the

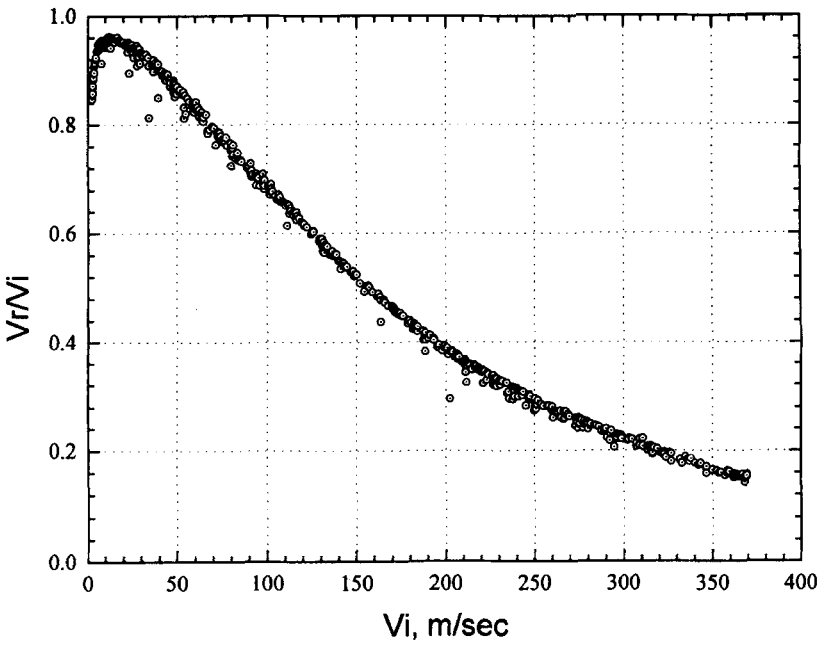

FIGURE 2 Magnitudes of $V_{r\infty}/V_{i\infty}$ *versus* $V_{i\infty}$ for 1.27 μm diameter polystyrene spheres striking a flat, fused-silica surface at normal incidence in vacuum. The V_r and V_i data were measured at large particle-surface separation, beyond the range of any expected interactions. A total of 763 data points is shown.

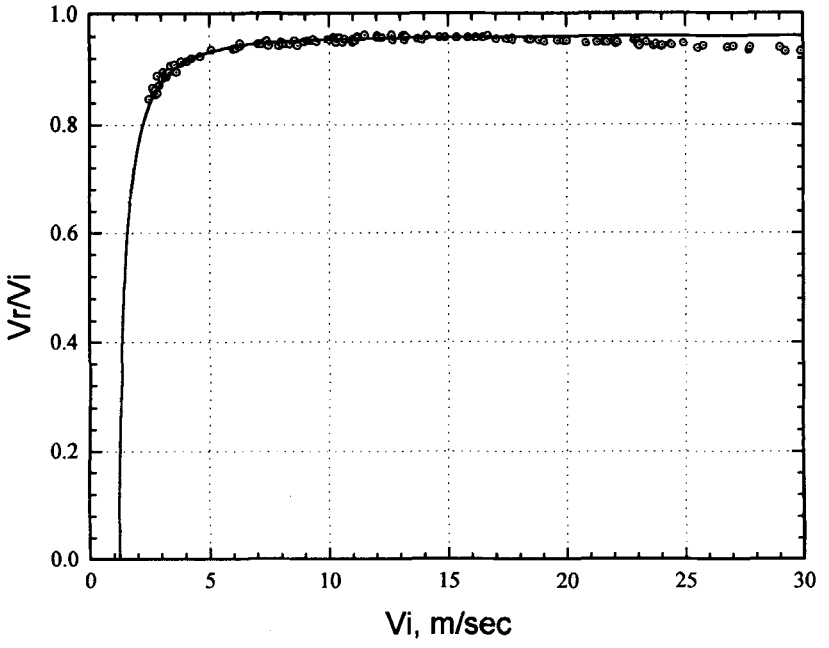

FIGURE 3 A magnified view of the low-$V_{i\infty}$ data of Figure 2. The curve is taken directly from fitted expression (11) of the text, giving intercept $V_{r\infty}/V_{i\infty} = 0$ at the capture-limit velocity $V^*_{i\infty} = 1.23$ m/sec.

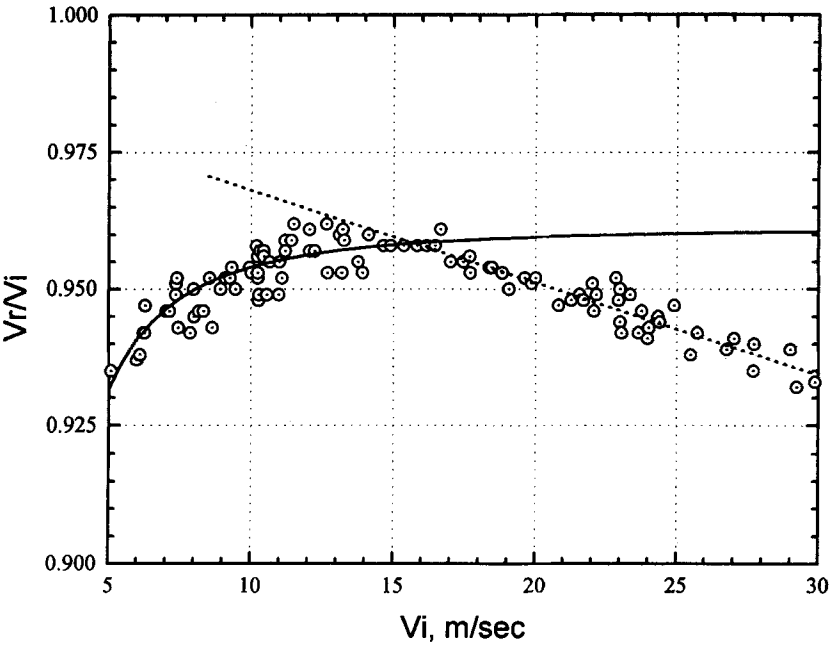

FIGURE 4 A more highly magnified view of the data of Figure 2. The data and solid curve diverge above $V_{i\varphi} = 16$ m/sec, apparently the impact velocity at onset of particle deformation. A fitted (dotted) line to the data above 16 m/sec is shown to identify the origin of divergence.

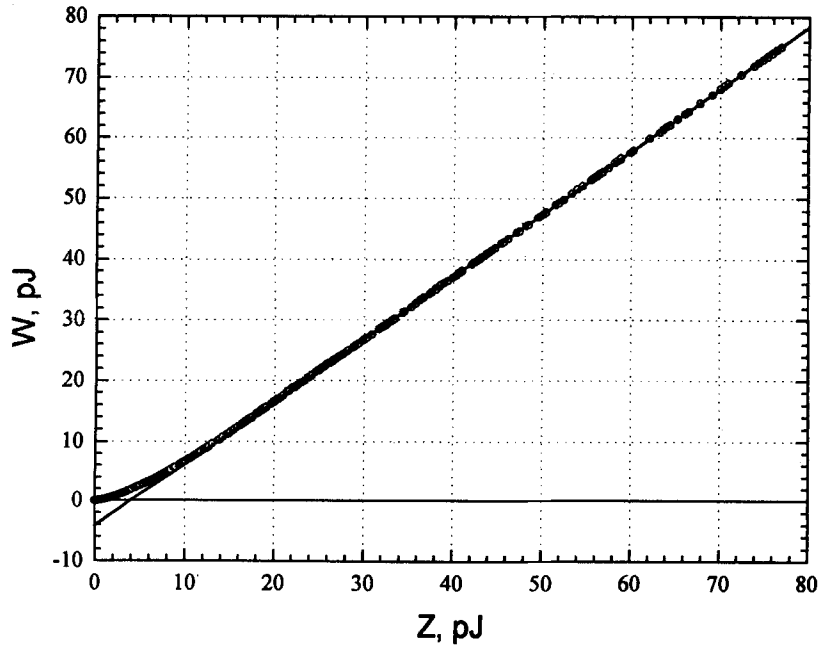

FIGURE 5 The 763 data points of Figure 2 plotted as kinetic energy dissipated during collision (W) *versus* incident kinetic energy (Z). The line $W(Z) = A + B \times Z$ was fitted to 145 data points over the range $Z \geq 27$ pJ giving coefficients $A = -4.180$ pJ and $B = 1.0322$.

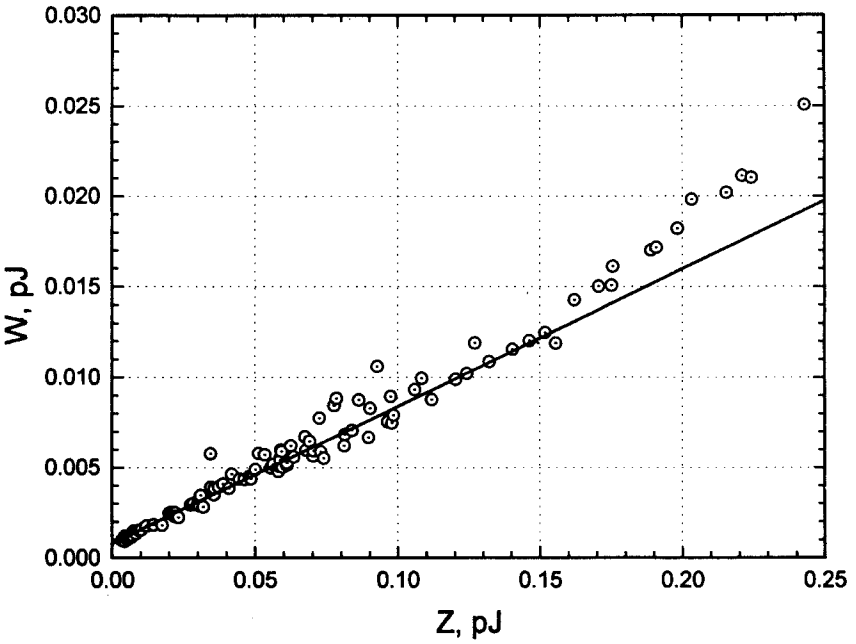

FIGURE 6 A magnified view of the data of Figure 5 showing the line $W(Z) = a + b \times Z$ with coefficients a and b (given in the text) obtained by a fit to 198 data points over the range $Z < 0.15$ pJ.

passages were sensed by a photo-multiplier tube and a pair of electronic time-marker pulses was generated at the passage of each particle in both the incident and rebound directions. The temporal separation of the pulses in a pulse pair, or the particle time-of-flight, was used with the known separation of the laser beams to obtain jointly both the $V_{i\infty}$ and $V_{r\infty}$ values for each particle, accurate to four significant figures at small values of $V_{i\infty}$.

A few days after cleaning, the target surface was observed to have a faint "hazy" appearance due, apparently, to a coating from particle impacts and possibly from other sources as well. The test chamber was pumped by a six-inch diffusion pump isolated by a liquid-air trap to prevent backstreaming of pump oil. Neither surface contamination of the particles or the target appeared to affect the data. Included in the 763 data points are points taken on 10 different days over several weeks using different particle-suspension preparations and after different intervals following recleaning of the target surface with clean methanol. No discontinuity or detectable shift in the data was detected.

Inherent to this measurement procedure, the particles were cooled during the adiabatic expansion to a temperature estimated[8] to be 30 K below the ambient temperature of 293 K. Subsequently, the particles were warmed during deceleration in the braking chamber. However, the extent of warming varied with particle residence time in the braking chamber and, therefore, with velocity $V_{i\infty}$. While the temperature shift is small, it is systematic with the lower velocity particles being no more than a few

degrees below room temperature and the higher velocity ones being up to 30 K below room temperature.

IV INTERROGATION OF THE MEASURED DATA BY USE OF THE MODEL

Consider a simple, normal-direction, particle-surface collision for which the total energy loss is $W = KE_{i\infty} - KE_{r\infty}$. For fixed composition of the particle-surface system and for fixed particle size, one parameter controls the collision dynamics, *viz.*, incident kinetic energy $KE_{i\infty} = Z$, which we regard as the independent variable in the single size- and composition-species particle and single target species collision process. Thus, several collision parameters are dependent on Z. To obtain the functional dependence of W on Z and on other parameters, we must first identify these parameters. From (1),

$$W = (Z - E_{io})(1 - e^2) - \Delta E_0, \tag{5}$$

so that $W = W(Z, E_{io}, e^2, \Delta E_0)$. To account for the W-dependencies, we write by the chain rule

$$dW/dZ = \partial W/\partial Z + \partial W/\partial E_{io} \times \partial E_{io}/\partial Z + \partial W/\partial e^2 \times \partial e^2/\partial Z + \partial W/\partial \Delta E_0 \times \partial \Delta E_0/\partial Z. \tag{6}$$

By a Taylor's series expansion, about any selected reference value, Z^*, .

$$W(Z) = W(Z^*) + (Z - Z^*) \times [dW/dZ]_{Z^*} + 1/2(Z - Z^*)^2 \times [d^2W/dZ^2]_{Z^*} + \ldots \tag{7}$$

At small $Z - Z^*$ the first two terms of (7) provide an adequate, linear approximation [such as the one fitted to the $Z < 0.15$ pJ data shown in Figure 6] for which case (6) and (7) give

$$W(Z) = W(Z^*) + (Z - Z^*) \times \{\partial W/\partial Z + \partial W/\partial E_{io} \times \partial E_{io}/\partial Z + \partial W/\partial e^2 \times \partial e^2/\partial Z + \partial W/\partial \Delta E_0 \times \partial \Delta E_0/\partial Z\}. \tag{8}$$

By (8) we see that the slope of the linear $W(Z)$ *versus* Z function (at low $Z < 0.15$ pJ data) is a sum of a constant plus a sum of four terms {in braces} which multiplies $(Z - Z^*)$.

We note that the second through fourth terms in braces of (8) can be written

$$(Z - Z^*) \times \partial W/\partial E_{io} \times \partial E_{io}/\partial Z = (E_{io} - E_{io}^*) \times \partial W/\partial E_{io}$$

$$(Z - Z^*) \times \partial W/\partial e^2 \times \partial e^2/\partial Z = (e^2 - e^{*2}) \times \partial W/\partial e^2$$

and $$(Z - Z^*) \times \partial W/\partial \Delta E_o \times \partial \Delta E_o/\partial Z = (\Delta E_o - \Delta E_o^*) \times \partial W/\partial \Delta E_o,$$

where E_{io}^*, e^{*2}, and ΔE_0^* are reference values corresponding to $Z = Z^*$. Substitution of these terms in (8) gives

$$W(Z) = W(Z^*) + (Z - Z^*) \times \partial W/\partial Z + (E_{io} - E_{io}^*) \times \partial W/\partial E_{io} + (e^2 - e^{*2}) \times \partial W/\partial e^2 + (\Delta E_0 - \Delta E_0^*) \times \partial W/\partial \Delta E_0. \tag{9}$$

Comparison of (9) and (5) gives

$$\partial W/\partial Z = 1 - e^2,$$

$$\partial W/\partial E_{io} = -(1 - e^2),$$

$$\partial W/\partial e^2 = -(Z - E_{io}),$$

and

$$\partial W/\partial \Delta E_o = -1.$$

The constant and all four terms in braces of (8) are now determined and we take for Z^* the value of Z at the capture-limit condition at which $W(Z^*) = Z^*$, by definition. We thus obtain in place of (9)

$$W(Z) = Z^* + (Z - Z^* - E_{io} + E_{io}^*) \times (1 - e^{*2}) - (Z - E_{io}) \times (e^2 - e^{*2}) - (\Delta E_o - \Delta E_o^*). \tag{10}$$

[As noted by one reviewer, (10) follows directly from (5) without use of a Taylor's series expansion, but inclusion of the expansion is thought to be useful.] When constant E_{io} or constant e^2 is [are both] assumed, quantity $(E_{io} - E_{io}^*) \times (1 - e^2)$ or $(Z - E_{io}) \times (e^2 - e^{*2})$ vanishes [both vanish] from (10).

For the case $Z^* < Z < 0.15$ pJ, (7) through (10) are valid and the data of Figure 6 fall near the straight-line, linear-least-squares fit of 155 data points in this $Z \leq 0.15$ pJ range. The fitted line is given by

$$W = a + b \times Z = 7.9162 \times 10^{-4}\,\text{pJ} + 0.075813 \times Z. \tag{11}$$

Comparison of (10) and (11) and assuming E_{io} and e^2 to be constants at small Z gives

$$Z^* \times e^{*2} - \Delta E_o^* = a = 7.9162 \times 10^{-4}\,\text{pJ} \tag{12}$$

and

$$\{(1 - e^2) - (Z - E_{io}) \times \partial e^2/\partial Z - \partial \Delta E_o/\partial Z\} = 0.075813. \tag{13}$$

We examine first the consequences of (13) and then those of (12).

In the linear range of $W(Z)$, no Z^2 term is significant and $\partial e^2/\partial Z$ must be small. Thus,

$$\partial \Delta E_o/\partial Z = 1 - e^2 - b = 0.0026 \pm 0.0017,$$

taking $e = 0.960$ (as fitted to the measured data of Fig. 3). The data are not adequate for resolution of a precise value of such a small quantity. We conclude that any variation in ΔE_0 for $Z < 0.15$ pJ falls within our sensitivity tolerance. Such a result is suggested by (5) and (11) which give

$$W(Z) = -[\Delta E_o + (1 - e^2) E_{io}] + (1 - e^2) Z = a + b \times Z. \tag{14}$$

The model and the assumptions used in fitting it to the data are consistent with the notion that the predominant Z-dependence of W at small Z is contained in the term of (14) having coefficient $b = (1 - e^2)$.

The capture-limit velocity, $V_{i\infty}^*$, is determined from $Z^* = m/2\ V_{i\infty}^{*2}$, where Z^* is determined by (11) and $Z^* = W(Z^*) = a/(1 - b) = 8.60 \times 10^{-4}$ pJ, giving capture-limit velocity $V_{i\infty}^* = 1.23$ m/sec.

A value of $\Delta E_o^* = E_{ro}^* - E_{io}^*$ is obtained from (12) using Z^* and $e^{*2} = 0.960^2 = 0.9216$, by which $-\Delta E_o^* = a - Z^* \times e^2 = a \times (1 - e^2 - b)/(1 - b) = 2.2 \times 10^{-6}$ pJ. This value appears to have the correct order of magnitude, *i.e.*, it is within one order of the Bradley-Hamaker-(BH) model prediction of $E_{io} = E_{BH} = 1.8 \times 10^{-5}$ pJ for an undeformed polystyrene sphere of 1.27 μm diameter on a fused-silica substrate. Even though the relative uncertainty of ΔE_o^* is large, we note that $\Delta E_o^* = E_{io}^* - E_{ro}^*$ may[1] have larger magnitude than E_{io}^* due to change in E (flattening) during collision,[2] be influenced by model dependence due to increase in x_{io} and/or x_{ro} to include all irreversible dissipation of collision energy, and[3] contain uncertainty due to long extrapolation from the Z values at which a and b are fitted to the Z^* intercept, an extrapolation quite apparent in the fitted curve of Figure 3. For this last reason, especially, we believe the uncertainty in coefficient a is much larger than in coefficient b.

Dahneke[3] and Hays and Wayman[4] reported E_{io} values fitted to their measured bounce data for 1.27 and 12 μm diameter polystyrene particles, respectively, to be $500 \times E_{BH}$ for the case $\Delta E_o = 0$. This result contradicts the model prediction that fitted E_o values are equal to or less than actual E_o values. However, the results are consistent with the model if $\alpha = \Delta E_o/[(1 - e^2) \times E_{io}] \gg 1$, as shown by rearranging (3)

$$\Delta E_o + (1 - e^2) \times E_{io} = mV_{i\infty}^2 \times [V_{r\infty}^2/V_{i\infty}^2 - e^2]/2. \tag{15}$$

If α were small, as assumed in the earlier analyses,[3,4] $E_{io} \gg E_{BH}$ in violation of the model. Thus, the assumption $\alpha = 0$ is invalid by the model. In the opposite case $\alpha \gg 1$, the model predicts a unique value of ΔE_o, *viz.*,

$$\Delta E_o = mV_{i\infty}^2 \times [V_{r\infty}^2/V_{i\infty}^2 - e^2]/2. \tag{16}$$

For the data considered in this study, the contribution of E_{io} can be ignored, as will be confirmed if the fitted result gives $\alpha \gg 1$. A fit of (16) to the $Z < 0.15$ pJ data of Figure 6 gives $-\Delta E_o = a = 7.92 \times 10^{-4}$ pJ $\cong 40 \times E_{BH}$ and $e = 0.9596$. Small E_{io} and small $(1 - e^2)$ values combine to give $\alpha \gg 1$ for the particle collision data analyzed here.

Another property that appears accessible to interrogation of measured data *via* the model is the impact energy at onset of material deformation, which may be used with a suitable quasi-stationary elasticity model to determine the elastic limit or yield stress of the particle-surface-material system. Measurement of this quantity is difficult for small-particle samples. Moreover, the elastic limit is known to be temperature and strain-rate dependent and particle-surface collision measurements allow control of temperature and strain rate over broad ranges. We note from Figure 6 that the linear range of $W(Z)$ *versus* Z extends up to a limit of $Z = 0.15$ pJ, corresponding to $V_{i\infty} = 16$ m/sec of Figures 3 and 4 at which value the $V_{r\infty}/V_{i\infty}$ *versus* $V_{i\infty}$ curve shows a distinct break in form. This transition point is believed by the author to coincide with the onset of particle deformation, where the value of e^2 should suddenly obtain a different functional form. The present theory may be extended to include a different functional form above the "onset-of-deformation" limit, whether it be plastic or a "transient dynamic" deformation, but we limit our present examination to the linear data range.

Analysis *via* the model of measured data beyond the linear range and use of the model to explore other parameter spaces will be addressed elsewhere. However, we

briefly consider the linear form of the *W versus Z* data at large Z, shown in Figure 5 with the fitted curve $W = A + B \times Z$, where $A = -4.180$ pJ and $B = 1.0322$. The mechanistic origin of the observed linear curve has not yet been established, but one possible cause is the influence of temporary or permanent (plastic) deformation beginning at $Z = 0.15$ pJ and increasing with Z. The curved transition range of Figure 5 showing increasing dW/dZ with increasing Z may be caused by flattening, with (nonlinear) increase in ΔE_o with Z responsible for the curvature. Once a particle is substantially flattened, continued nonlinear dependence of ΔE_o on Z would presumably be small and $W(Z)$ would again be linear in Z.

In the highest (linear) range of *W versus* impact energy measured, other dissipation mechanisms appear to become important and additive to the "low-energy" mechanisms such as energy radiation into the surface material. At high impact energy, all increase in impact energy is dissipated by breaking of bonds and exciting internal-energy modes of the particle-surface materials, *i.e.*, heating, melting, and vaporization of particle-surface material. Interestingly, additional energy dissipated exceeds additional collision energy in the high-energy range ($B = 1.0322 > 1$), perhaps due to a compound addition of melting, viscous flow, and associated increase in $-\Delta E_o$.

V CONCLUSIONS

Incident and rebound direction velocities of 1.27 μm diameter polystyrene spheres striking a polished, fused-silica surface at normal incidence in vacuum have been jointly measured over incident velocities between 2.5 and 380 m/sec. The data are tightly packed about a characteristic curve, which indicates existence of a reliable model. The simplest, most general model will almost certainly be based in the model parameter space (energy space) for which the characteristic curve is simplest (a line).

A semi-empirical model for simple, particle-surface collisions was fitted to the measured collision data to explore what mechanisms and properties of a particle-surface system might be determined.

The following properties were determined to varying levels of precision.[1] The low-impact-velocity coefficient of restitution $e = 0.960$,[2] the impact kinetic energy at onset of particle deformation $Z = 0.15$ pJ,[3] an increase in particle-surface-attractive-energy during collision $\Delta E_o = -7.9 \times 10^{-4}$ pJ was found, a value some 40 × that predicted by a BH-model calculation.

The second of these three properties might be used with a quasi-stationary, elasticity-theory model to determine an elastic yield stress for a particle-surface-material system. However, this possibility is tentative until it is established that the distinct break in the curve of Figure 4 corresponds to the onset of plastic yield and that a quasi-stationary elasticity theory can provide adequate approximations for a dynamic process.

The strategies and methods suggested here may help provide accurate characterization of particle-surface collisions and determination of mechanisms and properties which control them. They may also help establish an improved understanding of particle-surface adhesion force and energy. In pursuit of these goals, interrogation of measured data over a broader range of property spaces should be explored in future studies.

References

1. B. E. Dahneke, *J. Colloid and Interface Sci.* **37,** 342–353 (1971).
2. B. E. Dahneke, *Aerosol Sci. Technol.* (in press).
3. B. E. Dahneke, *J. Colloid and Interface Sci.* **51,** 58–65 (1975).
4. D. A. Hays and W. H. Wayman, in *Adhesion of Charged Particles,* Institute of Physics Conference, Poster Number 66 (1983).
5. S. Wall, W. John, H. Wang and S. Goren, *Aerosol Sci. Technol.* **12,** 926–946 (1990).
6. N. A. Burnham, R. J. Colton and H. M. Pollock, *J. Vac. Sci. Technol* **A9,** 2548–2556 (1991).
7. N. A. Burnham, R. J. Colton and H. M. Pollock, *Nanotechnology* **4,** 64–80 (1993).
8. B. E. Dahneke, "Cooling of Particles in Aerosol Beams," in *Rarefied Gas Dynamics,* K. Karamcheti, Ed. (Academic Press, New York, 1974), pp. 197–203.